Report

Cell Reports

The Transcriptional Repressor Polycomb Group Factor 6, PCGF6, Negatively Regulates Dendritic Cell Activation and Promotes Quiescence

Graphical Abstract

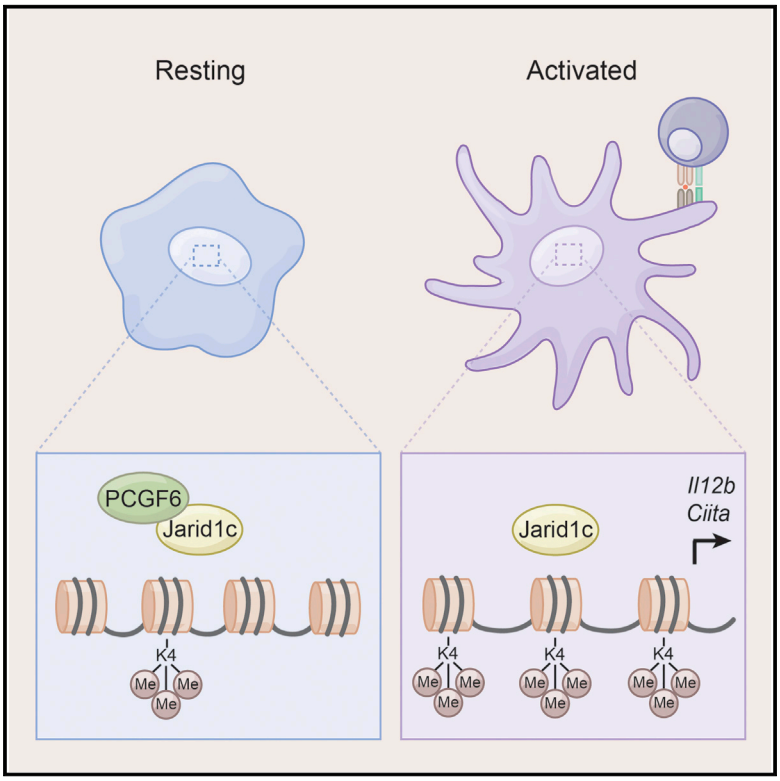

Authors

Giselle M. Boukhaled, Brendan Cordeiro, Genevieve Deblois, ..., Mathieu Lupien, John H. White, Connie M. Krawczyk

Correspondence

connie.krawczyk@mcgill.ca

In Brief

Boukhaled et al. identify PCGF6 and JARID1c as negative regulators of dendritic cell (DC) activation. PCGF6 was found to suppress chromatin accessibility and H3K4me3 levels of genes important for DC activation. PCGF6 interacts with JARID1c in DCs, and JARID1c is necessary, in part, for PCGF6-mediated suppression of DC activation.

Highlights

- The transcriptional repressor PCGF6 negatively regulates dendritic cell activation
- PCGF6 regulates H3K4me3 levels at genes important for dendritic cell function
- PCGF6 interacts with the histone demethylase JARID1c

Accession Numbers

GSE83640

Boukhaled et al., 2016, Cell Reports *16*, 1829–1837
August 16, 2016
http://dx.doi.org/10.1016/j.celrep.2016.07.026

CellPress

Cell Reports
Report

The Transcriptional Repressor Polycomb Group Factor 6, PCGF6, Negatively Regulates Dendritic Cell Activation and Promotes Quiescence

Giselle M. Boukhaled,[1] Brendan Cordeiro,[1] Genevieve Deblois,[2] Vassil Dimitrov,[3] Swneke D. Bailey,[2] Thomas Holowka,[4] Anisa Domi,[1] Hannah Guak,[1] Huai-Hsuan Clare Chiu,[1] Bart Everts,[5] Edward J. Pearce,[4] Mathieu Lupien,[2] John H. White,[3] and Connie M. Krawczyk[1,*]

[1]Goodman Cancer Research Center, Departments of Microbiology and Immunology and Physiology, McGill University, Montreal, QC H3G 1Y6, Canada
[2]The Princess Margaret Cancer Centre, University Health Network, Department of Medical Biophysics, University of Toronto, Toronto, ON M5G 1L7, Canada
[3]Department of Physiology, McGill University, Montreal, QC H3G 1Y6, Canada
[4]Department of Immunometabolism, Max Planck Institute of Immunobiology and Epigenetics, Faculty of Biology, University of Freiburg, Freiburg, Freiburg 79104, Germany
[5]Department of Parasitology, Leiden University Medical Center, Albinusdreef 2, Leiden 2333 ZA, the Netherlands
*Correspondence: connie.krawczyk@mcgill.ca
http://dx.doi.org/10.1016/j.celrep.2016.07.026

SUMMARY

Pro-inflammatory signals provided by the microenvironment are critical to activate dendritic cells (DCs), components of the innate immune system that shape both innate and adaptive immunity. However, to prevent inappropriate immune activation, mechanisms must be in place to restrain DC activation to ensure DCs are activated only once sufficient stimuli have been received. Here, we report that DC activation and immunogenicity are regulated by the transcriptional repressor Polycomb group factor 6 (PCGF6). *Pcgf6* is rapidly downregulated upon stimulation, and this downregulation is necessary to permit full DC activation. Silencing PCGF6 expression enhanced both spontaneous and stimulated DC activation. We show that PCGF6 associates with the H3K4me3 demethylase JARID1c, and together, they negatively regulate H3K4me3 levels in DCs. Our results identify two key regulators, PCGF6 and JARID1c that temper DC activation and implicate active transcriptional silencing via histone demethylation as a previously unappreciated mechanism for regulating DC activation and quiescence.

INTRODUCTION

Dendritic cells (DCs) play an essential role in host defense by recognizing invading pathogens, initiating inflammation, and stimulating the activation and differentiation of T cells, central mediators of the adaptive immune response. Key to the capacity of DCs to fulfill these functions is their ability to transition from a resting or quiescent state to an active state. A major pathway for DC activation is provided by pattern recognition receptors (PRRs) that recognize molecular patterns from microbes termed PAMPS/MAMPS (pathogen-associated molecular patterns/microbe-associated molecular patterns) and self-molecules termed DAMPS (damage-associated molecular patterns) (Hammer and Ma, 2013; Macagno et al., 2007; Mogensen, 2009).

Despite their diversity, all PRRs initiate signaling pathways that lead to coordinated changes in cellular biology necessary for the effector function of DCs, most of which are underpinned by broad changes in gene expression (Hammer and Ma, 2013; Johnson and Ohashi, 2013). DCs that have undergone activation enhance their antigen-presentation capacity, increase the expression of costimulatory molecules such as CD80 and CD86, and produce many cytokines, chemokines, and lipid mediators that shape the inflammatory microenvironment (Sallusto et al., 1995). While the pathways that promote transcriptional activation downstream of inflammatory and PRR signals are well described (Mäkelä et al., 2009; Mogensen, 2009; Yoshimoto et al., 1997), less is known about negative regulators that counter activation signals.

One way of reinforcing transcriptional states in immune cells is through reversible, gene-specific, post-translational modifications of histones (Wen et al., 2008b). Methylation of lysine 4 of histone 3 (H3K4) marks transcriptionally active and accessible genes (Dong et al., 2012; Muramoto et al., 2010). In DCs and macrophages, H3K4me3 has been reported to be important for IL-12p40 production following Toll-like receptor (TLR) activation (Foster et al., 2007; Wen et al., 2008a; Yu et al., 2015). Mechanistically, H3K4me3 can facilitate transcription by promoting the initiation and elongation of transcripts of H3K4me3-marked genes (Benayoun et al., 2014; Lauberth et al., 2013; Ruthenburg et al., 2007).

Polycomb group factor 6 (PCGF6) (also known as MBLR for Mel18 and Bmi1-like RING finger protein) is a member of the Polycomb group (PcG) family of transcriptional repressors (Akasaka et al., 2002; Lee et al., 2007; Sun et al., 2015; Yang et al., 2016; Zdzieblo et al., 2014). PCGF6 has been identified in Polycomb

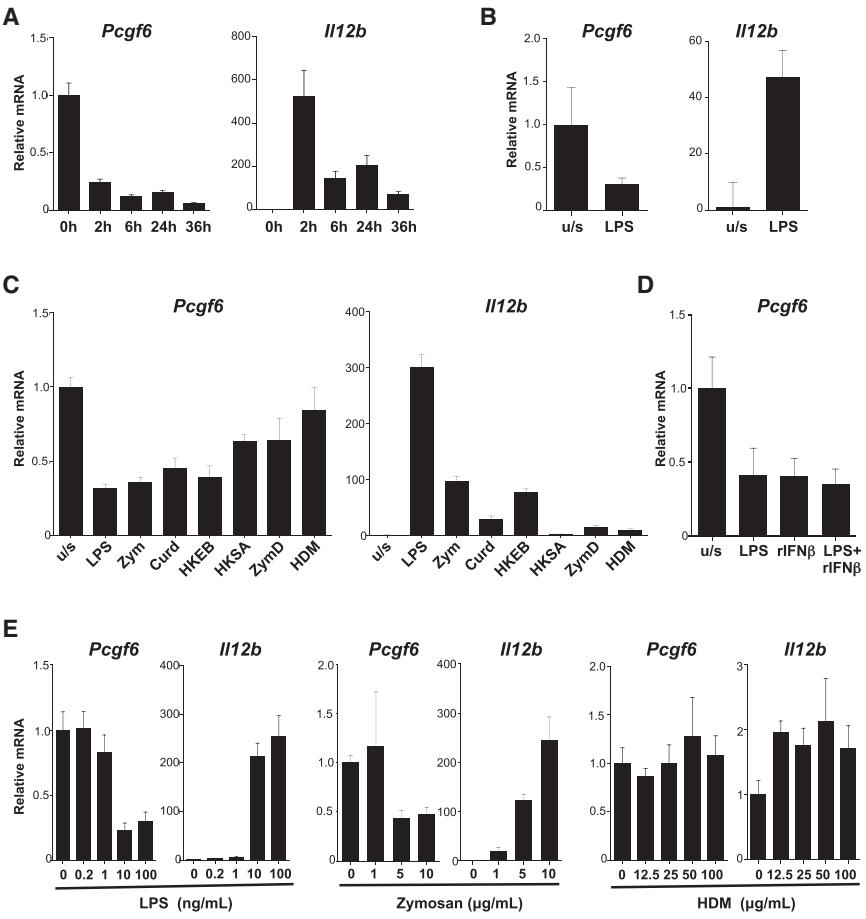

Figure 1. *Pcgf6* Expression Inversely Correlates with Activation Phenotype

(A–E) Gene expression of *Pcgf6* and *Il12b* in DCs stimulated with the indicated activators determined by qRT-PCR normalized to *Hprt*. Data are shown for one representative experiment of at least two to five independent experiments.

(A) DCs stimulated with LPS for the indicated times.

(B) Splenic DCs sorted from mouse spleens activated ex vivo with 10 ng/ml LPS for 4 hr.

(C) DCs stimulated with the indicated activators for 2 hr.

(D) DCs stimulated with the rIFNβ (1,000 U/ml) and/or LPS for 18 hr.

(E) DCs activated with indicated doses of stimuli for 18 hr.

LPS (lipopolysaccharide, 10 ng/ml); Zym (Zymosan, 10 μg/ml); Curd (Curdlan, 50 μg/ml); HKEB (heat-killed *Escherichia coli* B 10^7/ml); HKSA (heat-killed *Staphylococcus aureus* 10^7/ml); ZymD (Zymosan-depleted, 10 μg/ml); HDM (house dust mite, 50 μg/ml). See also Figure S1.

repressive complexes (PRC1) that have H3K9 methyltransferase and those that have H3K4 demethylase activity (Gao et al., 2012; Lee et al., 2007). PCGF6 has been reported to have a role in embryonic stem cell differentiation and male germ cell development (Sun et al., 2015; Yang et al., 2014; Zdzieblo et al., 2014); however, a function for PCGF6 in the biological context of DCs or any immune cell has not been reported.

Here, we show that PCFG6 is a negative regulator of DC activation and function and is integral to maintaining DC quiescence. Downregulation of PCGF6 expression accompanies, and is necessary for, DC activation by pro-inflammatory stimuli. We demonstrate that H3K4me3 levels in DCs are regulated both by PCGF6 and the histone demethylase JARID1c and that both proteins maintain a quiescent state. These findings identify two important negative regulators of DC activation and function and demonstrate that maintaining DC quiescence is an active process involving transcriptional silencing mechanisms.

RESULTS

Pcgf6 Is Expressed in Quiescent DCs and Downregulated following Activation

Pcgf6 was identified as being downregulated by lipopolysaccharide (LPS), a strong proinflammatory stimulant, in a previously performed microarray-based comparison of gene expression in quiescent versus activated DCs (Kane et al., 2004). Since Polycomb proteins are broadly known to regulate cellular gene expression programs in cells, we hypothesized that PCGF6 may repress gene expression at the steady state and that its downregulation following DC activation may favor increased transcription of the many genes that are coordinately expressed during DC activation. *Pcgf6* expression was characterized in DCs and was found to be rapidly downregulated as early as 2 hr post activation with LPS, coinciding with the induction of the proinflammatory cytokine *Il12b* (p40 subunit), and was maintained for up to 36 hr (Figure 1A). Importantly, *Pcgf6* was downregulated to a similar extent in splenic DCs and granulocyte-macrophage colony-stimulating factor (GM-CSF)-derived DCs (Figure 1B).

To determine whether *Pcgf6* downregulation was stimulant dependent, the expression of *Pcgf6* following exposure of DCs to a variety of stimulants was determined. *Pcgf6* expression inversely correlated with the extent of DC activation as measured by expression of CD80, CD86, and MHCII and induction of the inflammatory cytokine *Il12b* (Figures 1C, 1D, and S1). DCs activated by strong pro-inflammatory stimuli such as LPS, Zymosan, Curdlan, and interferon-β (IFN-β) reduced the expression of *Pcgf6* by 50%–90%, whereas weaker stimuli such as HDM and ZymD induced downregulation of *Pcgf6* expression to a lesser extent (Figure 1C). DCs were stimulated with titrated doses of select activators to determine whether the failure to downregulate *Pcgf6* was due to the dose and not the nature of the stimulus. Decreases in *Pcgf6* expression again correlated with the extent of DC activation (Figure 1E). These findings demonstrate that the transcriptional repressor *Pcgf6* is downregulated following DC stimulation and directly correlates with the activation status of DCs.

PCGF6 Maintains DC Quiescence by Negatively Regulating DC Activation

To test the hypothesis that the downregulation of PCGF6 permits, or facilitates, DC activation we used retroviral-mediated gene transfer to force continued expression of PCGF6 in DCs during activation (Figure S2A) (Krawczyk et al., 2008). Forced expression of PCGF6 resulted in decreased expression of CD80, CD86 and MHCII at steady state and following LPS-stimulation, which could not be rescued by increasing doses of stimuli (Figures S2B and S2C). DCs constitutively expressing PCGF6 also produced lower levels of proinflammatory cytokines, including interleukin 6 (IL-6), tumor necrosis factor α (TNF-α), and IL-12p40 (Figure 2A). Decreased production of IL-12p40 and IL-12p70 and expression of *Il12b* were also detected by ELISA and qRT-PCR, respectively (Figure 2B). This defect was not rescued by increasing the dose of LPS stimulation (Figure S2D). DCs derived from FLT3L-treated cultures overexpressing PCGF6 also produced less IL-12p40 following LPS activation (Figure S2E). Concomitant with DC activation is an increase in glycolysis to support the bio-energetic requirements of DC activation (Everts et al., 2014; Krawczyk et al., 2010). Consistent with a role for PCGF6 in suppressing DC activation, we found that DCs constitutively expressing PCGF6 had lower extracellular acidification rate (ECAR) (surrogate of glycolysis) following LPS stimulation (Figure 2C).

Interestingly, DCs that constitutively expressed PCGF6 produced more of the anti-inflammatory IL-10 both at rest and following LPS stimulation (Figures 2D and S2F). IL-10 antagonizes DC activation by suppressing the upregulation of activation markers and cytokines upon maturation (Corinti et al., 2001). However, neutralizing the IL-10R had no effect on PCGF6-mediated suppression of activation (Figures 2E and S2G). Furthermore, rIL-10 could not prevent *Pcgf6* downregulation (Figure 2F). These results suggest that PCGF6 and IL-10 operate in independent pathways to suppress DC activation.

To address the functional role of PCGF6 in DCs, the ability of transduced DCs to stimulate ovalbumin (OVA)-specific $CD4^+$ and $CD8^+$ TCR transgenic T cells (OT-II and OT-I) was examined. DCs with constitutive expression of PCGF6 were less efficient at inducing $CD4^+$ T cell activation, measured by CD44 and CD25 expression, proliferation, and Th1 differentiation (measured by IFN-γ production) (Figure 2G–2I). Likewise, DCs constitutively expressing PCGF6 were poor stimulators of $CD8^+$ T cell activation, proliferation and IFN-γ production in $CD8^+$ T cells (Figures 2J–2L).

In complementary experiments, PCGF6 expression was silenced by expressing a small hairpin RNA (shRNA) targeting PCGF6 (sh*Pcgf6*) (Figure S3A). DCs with reduced PCGF6 expression (sh*Pcgf6*) displayed increased levels of CD86 and MHCII in the resting state and following stimulation with LPS over a range of concentrations (Figures 3A and S3B). Likewise, silencing PCGF6 resulted in increased levels of IL-12p40 production both at rest and following activation (Figures 3B and 3C). A second hairpin targeting *Pcgf6* yielded similar results (Figures S3C–S3E). DCs with reduced PCGF6 expression derived from FLT3L-treated cultures displayed a phenotype similar to GM-CSF-derived DCs (Figure S3F). Both resting and LPS-activated DCs with reduced PCGF6 expression induced greater antigen-specific $CD4^+$ and $CD8^+$ T cell activation, as determined by CD44 and CD25 expression, proliferation, and IFN-γ production (Figures 3D–3I). These results indicate that PCGF6 expression is necessary for the maintenance of the resting state of DCs and that decreasing PCGF6 expression, even in resting DCs, is sufficient to stimulate stronger T cell responses.

Gene-Specific Regulation of Chromatin Accessibility and H3K4me3 Levels by PCGF6

Polycomb proteins are broadly known to regulate gene expression programs in cells, often through the regulation of histone modifications that influence chromatin structure and/or transcription (Schuettengruber et al., 2007). To examine changes in chromatin accessibility in the presence or absence of PCGF6, we used an assay for transposase-accessible chromatin (ATAC) to examine specific genes important for DC activation. ATAC libraries were generated from DCs transduced with either *Pcgf6* cDNA or sh*Pcgf6.* The accessibility of the promoters of *Ciita*, *H2-Ab1* (MHCII, IA^b), *Il12a, Il12b*, and *Actb* was examined using high-throughput sequencing data (Figures 4A and 4B) and validated by qRT-PCR on an independent set of samples (Figure S4). We observed decreased ATAC-qPCR enrichment relative to input at the promoters of *Ciita* and *Il12a* in DCs overexpressing PCGF6 (Figure S4), corresponding to reduced accessibility at these loci. An overall trend to decreased signal intensity by ATAC-sequencing (ATAC-seq) and relative enrichment by ATAC-qPCR was observed in PCGF6-overexpressing cells at the promoters of *Ciita*, *H2-Ab1, Il12a*, and *Il12b* (Figures 4A and S4). Conversely, there was a trend toward increased signal intensity by ATAC-seq and relative enrichment by ATAC-qPCR observed at these promoters upon depletion of PCGF6 (Figure 4B).

Since PCGF6 has been found in complexes with H3K4 demethylase activity (Lee et al., 2007), we examined whether PCGF6 could regulate H3K4me3 levels in DCs. We first examined whether changes in *Pcgf6* expression correlated with changes in H3K4 methylation in DCs using flow cytometry. We specifically gated on LPS-stimulated cells that were either IL-12p40^{hi}MHCII^{hi} or IL-12p40^{low}MHCII^{low} and compared the fluorescence intensity (Figure 4C). Consistent with its role as an activating epigenetic signature, we observed a positive correlation between the extent of H3K4me3 and the degree of cellular activation. Ectopic PCGF6 expression resulted in a decrease in H3K4me3 in both resting and LPS-stimulated DCs (Figure 4D), indicating that PCGF6 promotes H3K4 demethylation in DCs.

We examined H3K4me3 levels at the promoters of *Ciita*, *H2-Ab1*, *Il12a*, and *Il12b* using α-H3K4me3 chromatin immunoprecipitation (ChIP) qPCR (Figure 4E). We found a significant decrease in the enrichment of H3K4me3 at these promoters upon ectopic expression of PCGF6 and an increase in H3K4me3 enrichment with *Pcgf6* knockdown (Figure 4E). Levels of H3K4me3 were not significantly changed at the *Actb* promoter.

Maintenance of DC Quiescence by PCGF6 Is Dependent on JARID1c

PCGF6 was shown to be associated with and promote the histone demethylase activity of JARID1d, a histone demethylase

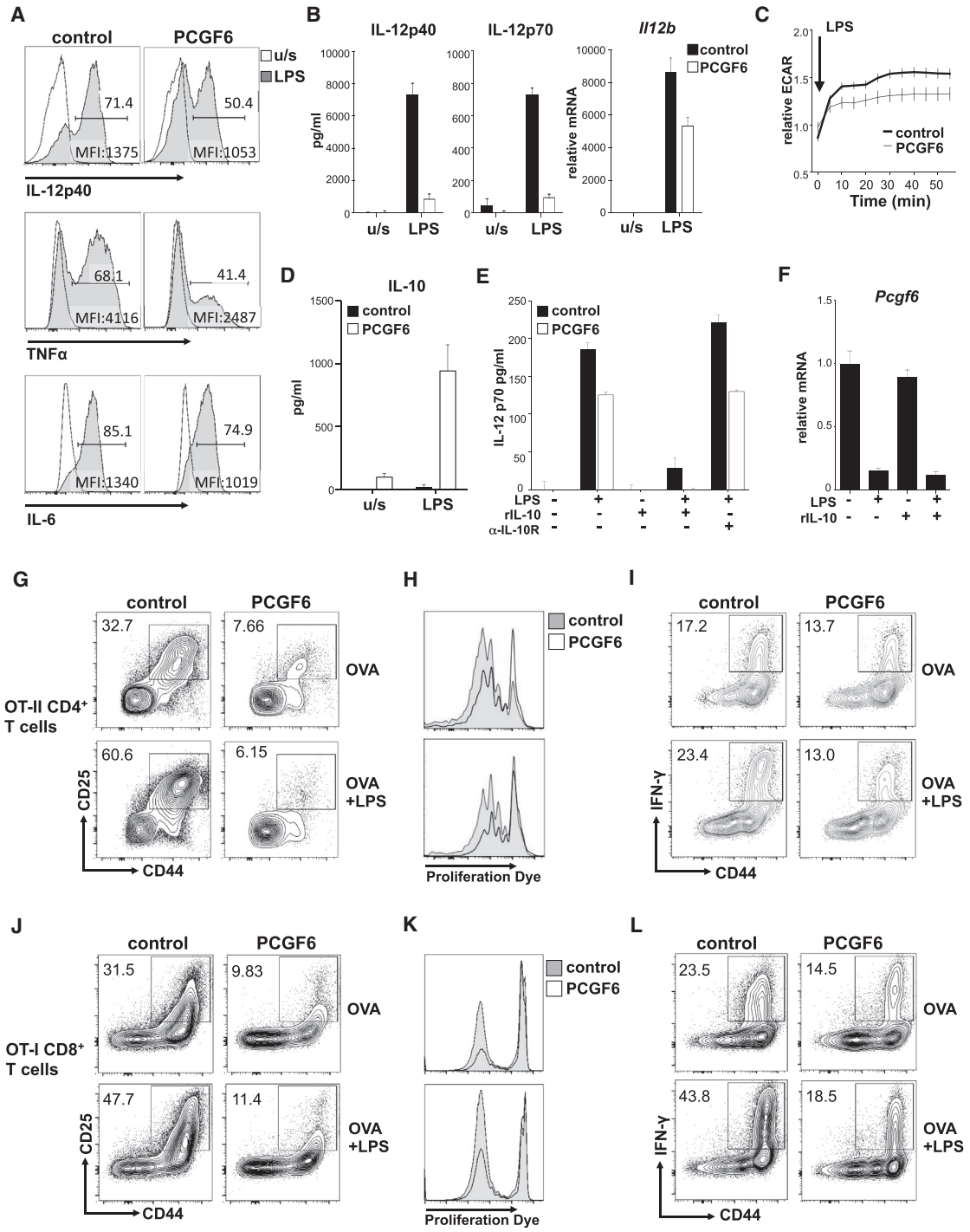

Figure 2. PCGF6 Negatively Regulates DC Activation

(A) DCs transduced with MSCV-based retrovirus (control) or virus expressing *Pcgf6* cDNA (PCGF6) were stimulated for 6 hr and stained intracellularly for the indicated cytokines. Plots show cells that are transduced (gated on hCD8 reporter). Frequency of gated events and the geometric mean fluorescence intensity (geoMFI) of the gated cells (bottom right) are indicated.

(B) Secreted IL-12p40 and IL-12p70 and expression of *Il12b* following 18-hr stimulation with LPS.

(C) Real-time ECAR (mpH/min) of transduced DCs during LPS stimulation (100 ng/ml) measured by a Seahorse bioanalyzer. Error bar represents SEM.

(D) IL-10 secretion and expression levels were determined as in (B).

(E) IL-12p70 production by transduced DCs stimulated with LPS ± rIL10 (20 ng/ml) or anti-CD210 (10 μg/ml) for 18 hr.

(F) *Pcgf6* and *Il12b* expression in DCs stimulated with LPS ± rIL-10.

(legend continued on next page)

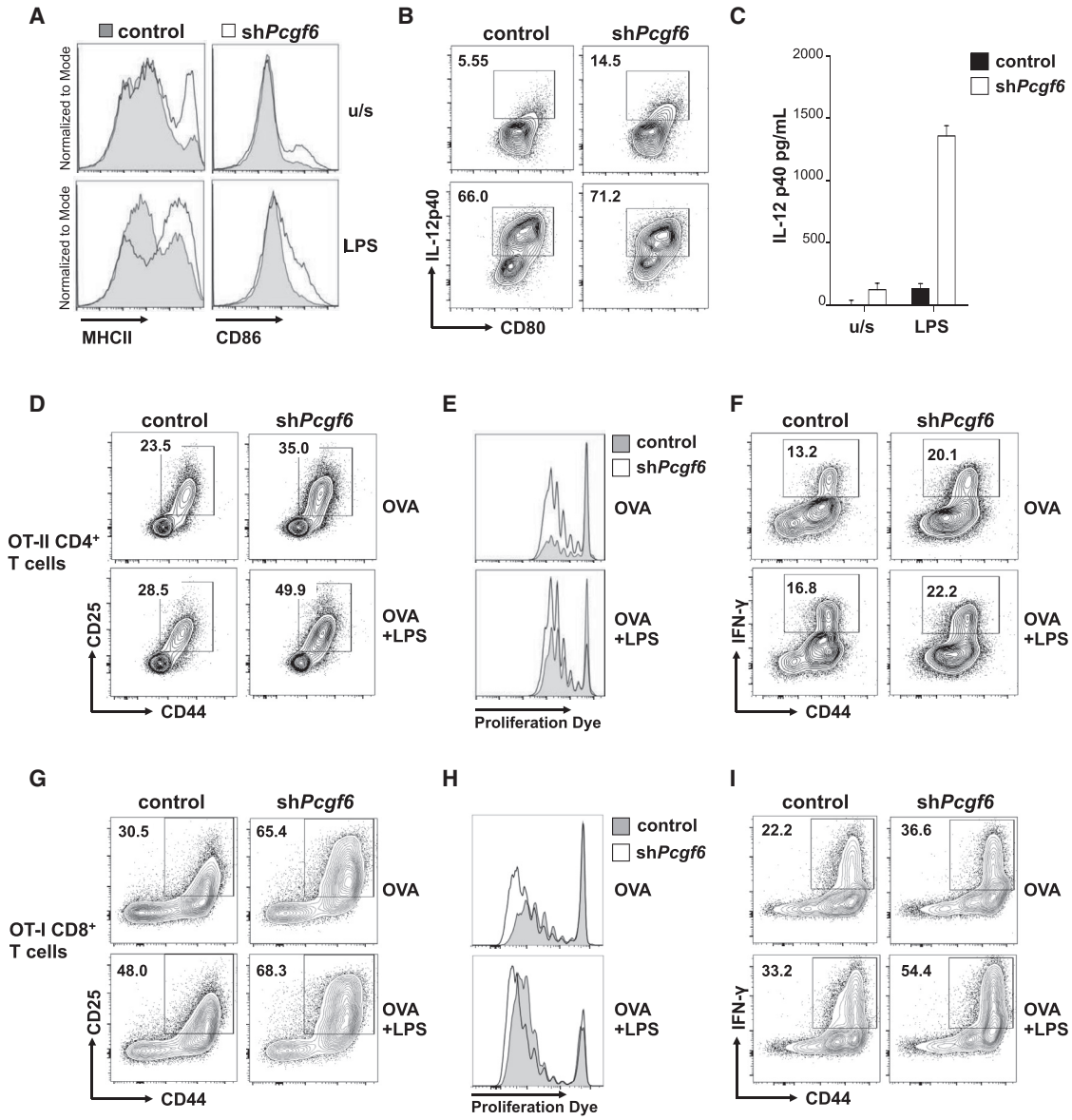

Figure 3. PCGF6 Regulates Both the Resting and Activated States of DCs

(A and B) MHCII, CD86 and IL-12p40 expression in DCs transduced with an shRNA targeting PCGF6 (sh*Pcgf6*) or empty vector (control) at rest and following stimulation with LPS for 6 hr. Plots show transduced (hCD8$^+$) cells.

(C) Secreted levels of IL-12p40 following 18 hr of LPS stimulation.

(D–I) CD4$^+$ and CD8$^+$ T cell co-culture experiments were performed as in Figure 2. Data are representative of three to five independent experiments. See also Figure S3.

that acts on H3K4me2 and H3K4me3 (Lee et al., 2007). Because our studies were performed with DCs from female mice that do not express the Y-linked JARID1d, we focused our attention on the X-linked homolog, JARID1c, another H3K4 demethylase (Outchkourov et al., 2013). PCGF6 and JARID1c were found to interact in DCs by co-immunoprecipitation (Figure 5A).

(G–L) Sorted transduced DCs were pulsed with ovalbumin protein ± LPS for 6 hr. Following stimulation, DCs were co-cultured with CD4$^+$ OTII T cells or CD8$^+$ OTI T cells that were labeled or not with proliferation dye.

(G, H, J, and K) 3–4 days after co-culture, the extent of T cell activation and proliferation was measured by CD25 and CD44 expression and proliferation dye dilution, respectively. Shown are CD4$^+$CD44$^+$ cells (H) and CD8$^+$ cells (K).

(I and L) 4–5 days after co-culture, T cells were stimulated for 4 hr with PMA and ionomycin and stained intracellularly for IFN-γ.

Unless otherwise indicated, error bars represent error calculated by SD of two or three replicates. Data are representative of at least three independent experiments. See also Figure S2.

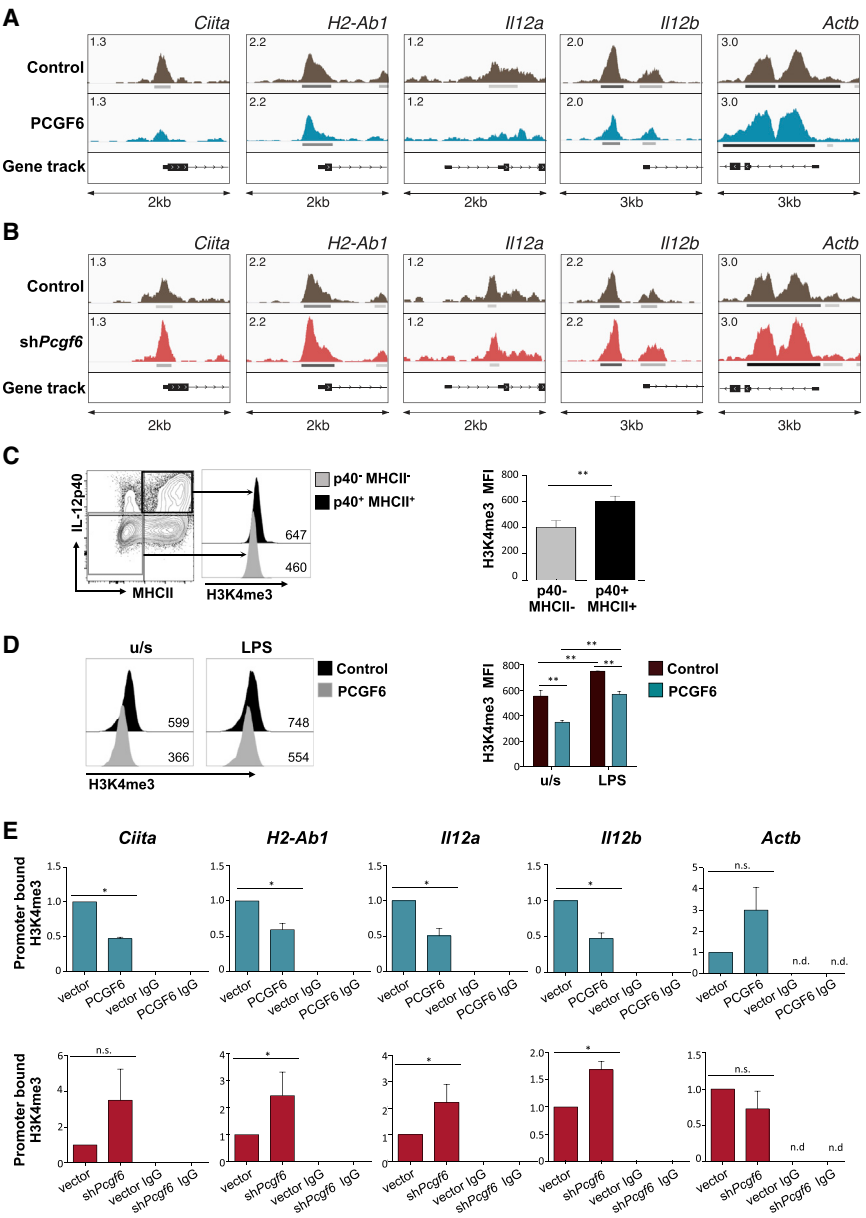

Figure 4. PCGF6 Suppresses H3K4me3 Levels in Resting and Activated DCs

(A and B) ATAC-seq of transduced resting DCs. Screenshot from a genome browser of peaks generated by ATAC-seq observed in proximity to the indicated genes. Peaks are a pileup of sequence alignments over the specified regions resulting from the ATAC reaction. The number in the top left of each panel represents the scale of the signal intensity. Called peaks are indicated by the shaded rectangles, where darkness of the rectangle represents relative intensity of the signal.

(C) DCs activated with LPS for 6 hr were stained intracellularly for MHCII, IL-12p40 (left), and H3K4me3 levels (right) and analyzed by flow cytometry. Inset values are the geoMFI of the adjacent histogram.

(D) H3K4me3 levels determined by flow cytometry in resting and LPS-stimulated DCs. GeoMFI is quantified on the right panel.

(C and D) Error bars represent SD of triplicate samples.

(E) ChIP of H3K4me3 in transduced DCs followed by qPCR of the promoters of indicated genes. ChIPs were performed on three biological replicates. Error bars indicate the SEM of pooled qPCR values from three independent ChIP experiments. $^{*}p < 0.05$, $^{**}p < 0.005$. See also Figure S4.

Unlike PCGF6, *Jarid1c* expression increased slightly (~2-fold) in response to LPS stimulation (Figure S5A). DCs expressing JARID1c-specific shRNA (sh*Jarid1c*) had increased levels of H3K4me3 (Figures 5B and S5B), consistent with the role of JARID1c as a histone demethylase in DCs.

Similar to cells expressing *Pcgf6*-specific shRNAs, expressing sh*Jarid1c* in DCs led to increased CD80, MHCII, and Il-12p40 levels both at rest and in response to LPS stimulation (Figures 5C and 5D). To examine whether JARID1c activity was needed for PCGF6-mediated suppression, we co-expressed PCGF6 and sh*Jarid1c* (Figure 5E). In the absence of JARID1c, PCGF6 was only partially able to suppress the expression of costimulatory molecules and IL-12p40 production (Figure 5F). Furthermore, PCGF6 could not suppress *H2-Ab1* and *Ciita* mRNA levels to the same extent in the absence of JARID1c (Figures 5G and S5C). Together, these data demonstrate that PCGF6 and JARID1c work in concert to negatively regulate the expression of key genes involved in DC activation and that JARID1c is required in part for PCGF6-mediated suppression.

DISCUSSION

Controlled activation of DCs is necessary to prevent the inappropriate induction of inflammation and activation of T cell responses, resulting in immunopathology and/or autoimmunity. Thus, it is important that the induction of the proinflammatory phenotype be restrained until sufficient, and appropriate, stimuli have been received. The maintenance of DC quiescence and the transition to activation are dynamic processes that require the coordinated induction of many genes necessary for their effector function. Here, we have identified two transcriptional repressors, PCGF6 and JARID1c, which cooperate to suppress the expression of genes that are associated with DC activation. Our work contributes to emerging evidence that maintaining the resting state in DCs is an active process involving negative regulators of transcription (Huang et al., 2012; Johnson and Ohashi, 2013). Our data also reveal that expression of PCGF6 must be downregulated to permit full activation of genes necessary for the acquisition of effector function of DCs in response to proinflammatory stimuli.

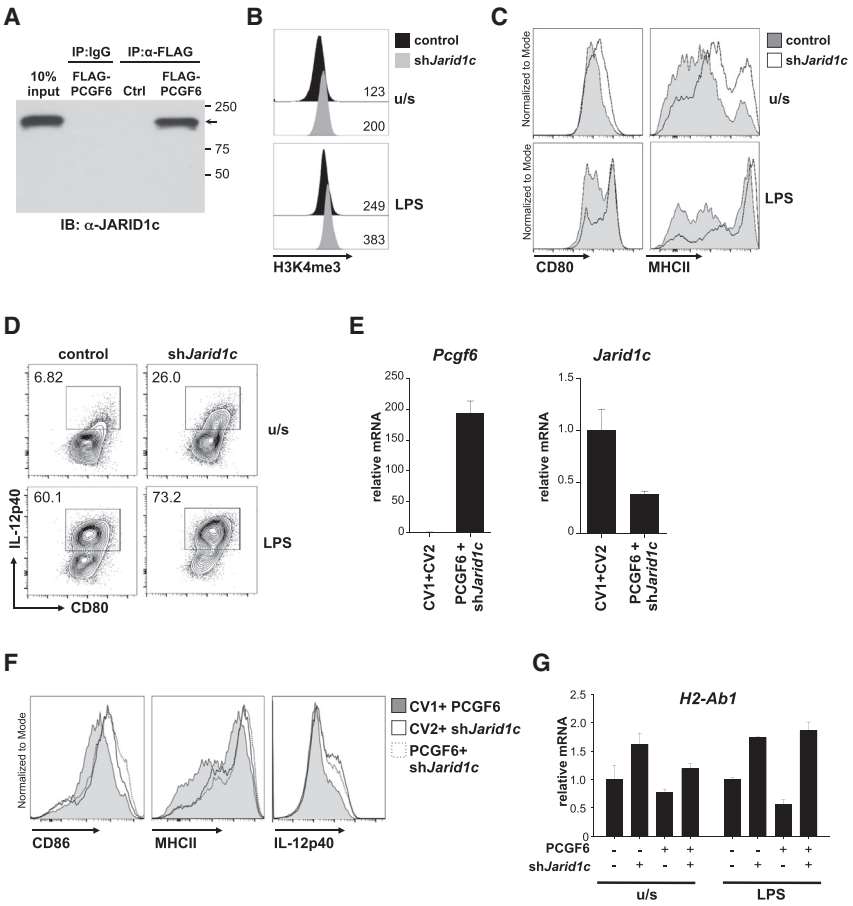

Figure 5. PCGF6 Negatively Regulates DC Activation in Part through JARID1c

(A) Immunoprecipitation (IP) performed on lysates from transduced DCs immunoblotted with anti-JARID1c.

(B) DCs transduced with a control vector or sh*Jarid1c* were activated with LPS for 6 hr. H3K4me3 levels were measured by flow cytometry.

(C and D) Transduced DCs treated as in (B) were assayed for surface marker expression and intracellular cytokine production (gated on $hCD8^+$ cells).

(E–G) DCs were transduced on days 1 and 2 of culture with either a relevant control vector (CV) or one expressing sh*Jarid1c* or PCGF6.

(E) Expression of *Pcgf6* and *Jarid1c* in double-transduced DCs measured by qRT-PCR and normalized to *Hprt*.

(F) Expression of MHCII, CD86, and intracellular IL-12p40 on human $CD8^+$ cells.

(G) Expression of *H2-Ab1* mRNA in transduced DCs.

Shown are data from one representative experiment out of three different experiments.

See also Figure S4.

DCs are poised to respond rapidly to their environment, and one mechanism to facilitate rapid responses could be transcriptional readiness, wherein the locus is primed and awaiting the arrival of activated transcription factors. Based on the ATAC experiments performed, the promoters of genes important for DC activation and function are relatively "open" at rest, in line with the need to have them immediately transcribed following PRR signaling. We found that expression levels of PCGF6 affected the "openness" of these promoters. While there are many chromatin modifications that can affect chromatin structure, we focused on H3K4me3 given the association of H3K4me3 with transcriptional activation and the published report that PCFG6 can interact with the H3K4 demethylase JARID1d (Lee et al., 2007). We found that H3K4me3 levels are increased in highly activated cells ($MHCII^{hi}p40^{hi}$) compared to immature cells and that PCGF6 expression decreased the global signal of H3K4me3. We specifically analyzed promoters of genes important for DC activation and found that PCGF6 expression decreases the level of H3K4me3 at these promoters. Mechanistically, we demonstrate that PCGF6 can associate with JARID1c and that the suppressive activity of PCGF6 in DCs is, in part, dependent on JARID1c. PCGF6 can also promote the transcription of genes such as IL-10, but the net effect of PCGF6-mediated regulation of gene expression is to dampen DC activation and promote a more quiescent state.

Active maintenance of the quiescent state is important for the fine-tuning of DC responses to a range of stimuli that have the potential to activate DCs. Here, we provide evidence that the extent to which these activating signals translate into transcriptional activation is tempered by negative regulators of transcription such as PCGF6 and JARID1c. PCGF6 and JARID1c antagonize mRNA expression by regulating H3K4me3 levels and in doing so promote a quiescent phenotype. In the absence of JARID1c and PCGF6, DCs are more active at rest, and at least for PCGF6, stimulate enhanced T cell responses. Therefore maintenance of the quiescent state via transcriptional repression in DCs has important consequences for the induction of both innate and adaptive immune responses.

Our findings demonstrate that PCGF6 and JARID1c regulate DC activation and function by actively suppressing H3K4me3 levels. These data support emerging evidence that constitutive inhibitory mechanisms are in place to regulate DC quiescence and temper activation. In the case of PCGF6, the expression of these factors must be downregulated to permit DC activation and subsequent triggering of adaptive immunity.

EXPERIMENTAL PROCEDURES

Mice and Reagents

C57BL/6 (Charles River Laboratories). OTII transgenic (Jackson 004194) and OTI (Jackson 003831) mice were maintained under specific-pathogen-free conditions at McGill University. All procedures were carried out in accordance with guidelines of the Canadian Council on Animal Care, as approved by the Animal Care Committee of McGill University. DC activators included LPS (*Escherichia coli* serotype 0111:B4) (Sigma-Aldrich), HDM (low endotoxin, Greer laboratories), Zymosan and Zymosan depleted of TLR ligands (Invivogen). Cytokines included GM-CSF, IL-10, and IFN-β (Peprotech). A $CD4^+$

and CD8$^+$ T cell negative selection kit (STEMCELL Technologies), Pan-DC enrichment kit, and phycoerythrin (PE)-positive selection kit (Miltenyi Biotec) were used. Antibodies are listed in Table S1. ELISA Ready-set-go kits: IL-12/23 p40, IL-12 p70, and IL-10 (eBioscience). Media reagents were RPMI (Corning, Thermo Fisher Scientific), Iscove's modified Dulbecco's media, fetal calf serum (FCS), L-glutamine and penicillin/streptomycin (Wisent), and non-essential amino acids (Gibco, Invitrogen).

Bone-Marrow Derived Dendritic Cells Culture and Transduction

Bone marrow cells were cultured and stimulated as described (Krawczyk et al., 2008). For intracellular staining bone-marrow derived dendritic cells (BMDCs) were incubated with brefeldin for 2 hr before the end of stimulation then fixed and permeabilized (eBioscience kit). Flt3L-derived BMDCs were generated as above using media containing 20% conditioned supernatants from a B16 cell line expressing FLT3L in place of GM-CSF. BMDC cultures were transduced as described using retrovirus produced in 293Ts transfected with either mouse stem cell virus (MSCV) or LMP-based (Krawczyk et al., 2008; Paddison et al., 2004) retroviral vectors using Lipofectamine 2000.

Gene Expression

RNA was extracted (Trizol) and cDNA was generated to perform SYBR-based qRT-PCR (For primers, see Table S2). Relative fold change was calculated using the $\Delta\Delta C_q$ method. The SD of triplicate samples was combined with the SD of the reference gene by error propagation. The range of fold change was then calculated by the formula $2^{(-\Delta\Delta Cq \pm s)}$, and the SD of the range in fold change represents the error bars indicated in the qPCR bar graphs.

Splenic DC Preparation and Ex Vivo Activation

Spleens from C57BL/6 mice were treated with collagenase and DNase for 20 min at 37°C and homogenized through a 70-μm filter, and red blood cells were lysed with ammonium chloride solution (150 mM NH_4Cl, 10 mM Tris, [pH 7]). DCs were isolated from total splenocytes by MACS pan-DC enrichment according to the manufacturer's protocol.

Seahorse Assay

Seahorse Extracellular Flux Analyzer was used to measure ECAR (mpH/min) following LPS stimulation. Briefly, sorted DCs were plated in six replicates in seahorse media freshly supplemented with 10% FCS, 2 mM L-Glutamine, 25 mM Glucose and 300 nM NaOH (pH adjusted to 7.4). LPS was injected directly by the Seahorse (final concentration, 100 ng/ml) measurements of ECAR were recorded every 5 min.

DC-T Cell Co-culture

2×10^4 sorted DCs were stimulated or not with LPS (10 ng/ml) and whole OVA protein (2 μg/ml) per well in 96-well plates. 6 hr following stimulation, 2×10^5 sorted CD4$^+$ T cells from OTII mice were added (1:10 ratio). On day 3 or 4, T cells were examined for proliferation (pre-labeled with CFSE or e450 Proliferation Dye) and expression of cell-surface activation markers. To detect cytokine production by intracellular staining, cells were stimulated for 4 hr with phorbol 12-myristate 13-acetate (PMA) (50 ng/ml) and ionomycin (500 ng/ml). For CD8$^+$ co-cultures, 1×10^4 sorted DCs were stimulated or not with LPS (0.5 ng/ml) and whole OVA protein (1 μg/mL) in 96-well plates and co-cultured and analyzed as described above.

H3K4me3 Staining and Chromatin Immunoprecipitation

To detect intracellular H3K4me3, cells were fixed with 4% PFA for 20 min at room temperature and washed and permeabilized with 100% methanol at 4°C for at least 30 min. Cells were then washed and stained at 4°C. ChIP was performed essentially as described in (Memari et al., 2015) with modifications detailed in Supplemental Experimental Procedures. Briefly, cells were cross-linked and lysed to obtain nuclei. Nuclei were lysed with sonication and chromatin was used for overnight immunoprecipitation (IP) at 4°C. Immunoprecipitated DNA was used as a template for qPCR specific to the promoter region of the indicated genes. Statistical significance was determined by an unpaired t test.

ATAC-Seq

ATAC-seq libraries from transduced DCs were sorted by fluorescence-activated cell sorting (FACS) for high hCD8, CD11c$^+$ cells and were prepared as previously described (Buenrostro et al., 2013) using 5×10^4 cells per sample and 50 ng DNA per input. Library preparation was achieved with DNA Library Preparation Kit (Illumina), and fragments were size-selected using Caliper LabChIP system (PerkinElmer). Reads were aligned to the Mouse genome (mm10) using Burrows-Wheeler Alignment tool (BWA) (Li and Durbin, 2009). Duplicate reads were marked and removed using Picard (https://github.com/broadinstitute/picard). For comparisons, the larger dataset was down-sampled to match the size of smaller dataset using Picard (https://github.com/broadinstitute/picard). Peaks were called using MACS2.0 (https://github.com/taoliu/MACS/) (Zhang et al., 2008) For ATAC-qPCR, ATAC libraries were prepared from three independent biological replicates as described above and used in real-time qPCR using the same primers listed for ChIP-qPCR. The fold enrichment relative to input was normalized to a negative control region.

Co-immunoprecipitation

Cell lysates from transduced DCs were prepared using RIPA lysis buffer (150 μM NaCl, 5 mM EDTA, 50 mM Tris [pH 5], 10% NP-40, 0.5% sodium deoxycholate, and 0.1% SDS) with protease inhibitor cocktail tablets (Roche). The lysates (1 mg) were cleared then incubated with beads pre-coated with either anti-FLAG M2 or normal mouse IgG for 2 hr. The beads were washed, and the proteins were eluted by boiling and processed for western blot using anti-JARID1c. 10% input (100 μg) was loaded as a control.

Statistical Analysis

Statistical analysis was performed using Prism 6.0b software and/or Microsoft Excel. Statistical significance was determined by unpaired t tests and indicated (n.s., not significant; *$p < 0.05$; **$p < 0.05$). Error bars represent either SD or SEM as described in the figure legends.

ACCESSION NUMBERS

The accession number for the ATAC-sequencing data reported in this paper is GEO: GSE83640.

SUPPLEMENTAL INFORMATION

Supplemental Information includes Supplemental Experimental Procedures, five figures, and three tables and can be found with this article online at http://dx.doi.org/10.1016/j.celrep.2016.07.026.

AUTHOR CONTRIBUTIONS

Conceptualization, C.M.K. and G.M.B.; Methodology, C.M.K., G.M.B., G.D., and V.D.; Validation, G.M.B., B.C., A.D., and H.G.; Formal Analysis, S.D.B. and G.D.; Investigation, C.M.K., G.M.B., B.C., G.D., V.D., T.H., A.D., H.G., H-H. and C.C.; Resources, J.H.W. and M.L.; Data Curation, G.D.; Writing Original Draft, C.M.K. and G.M.B.; Writing – Review & Editing, C.M.K., G.M.B., J.H.W., and M.L.; Visualization, C.M.K. and G.M.B.; Supervision, C.M.K., E.J.P., M.L., and J.H.W.; Project Administration, C.M.K. and G.M.B.; and Funding Acquisition, C.M.K.

ACKNOWLEDGMENTS

The authors thank Benedeta Hasaj, Kristin Hunt, Caitlyn Hui, Alborz Borjian, Fanny Guimont-Desrochers, and Drs. Julie St. Pierre and Russell Jones for critical analysis of the data and thoughtful discussions. We thank Drs. R. Jones and Martin Richer for critical reading of the manuscript. This work could not have been carried out without the service of Camille Stegen and Julien Leconte at the Duff and Cell Vision Flow Cytometry Facilities, respectfully. The work described here was supported by Canadian Institutes of Health Research (CIHR) grant MOP-126184 to C.M.K.

Received: July 6, 2015
Revised: May 25, 2016
Accepted: July 13, 2016
Published: August 4, 2016

REFERENCES

Akasaka, T., Takahashi, N., Suzuki, M., Koseki, H., Bodmer, R., and Koga, H. (2002). MBLR, a new RING finger protein resembling mammalian Polycomb gene products, is regulated by cell cycle-dependent phosphorylation. Genes Cells *7*, 835–850.

Benayoun, B.A., Pollina, E.A., Ucar, D., Mahmoudi, S., Karra, K., Wong, E.D., Devarajan, K., Daugherty, A.C., Kundaje, A.B., Mancini, E., et al. (2014). H3K4me3 breadth is linked to cell identity and transcriptional consistency. Cell *158*, 673–688.

Buenrostro, J.D., Giresi, P.G., Zaba, L.C., Chang, H.Y., and Greenleaf, W.J. (2013). Transposition of native chromatin for fast and sensitive epigenomic profiling of open chromatin, DNA-binding proteins and nucleosome position. Nat. Methods *10*, 1213–1218.

Corinti, S., Albanesi, C., la Sala, A., Pastore, S., and Girolomoni, G. (2001). Regulatory activity of autocrine IL-10 on dendritic cell functions. J. Immunol. *166*, 4312–4318.

Dong, X., Greven, M.C., Kundaje, A., Djebali, S., Brown, J.B., Cheng, C., Gingeras, T.R., Gerstein, M., Guigó, R., Birney, E., and Weng, Z. (2012). Modeling gene expression using chromatin features in various cellular contexts. Genome Biol. *13*, R53.

Everts, B., Amiel, E., Huang, S.C.-C., Smith, A.M., Chang, C.-H., Lam, W.Y., Redmann, V., Freitas, T.C., Blagih, J., van der Windt, G.J.W., et al. (2014). TLR-driven early glycolytic reprogramming via the kinases TBK1-IKKε supports the anabolic demands of dendritic cell activation. Nat. Immunol. *15*, 323–332.

Foster, S.L., Hargreaves, D.C., and Medzhitov, R. (2007). Gene-specific control of inflammation by TLR-induced chromatin modifications. Nature *447*, 972–978.

Gao, Z., Zhang, J., Bonasio, R., Strino, F., Sawai, A., Parisi, F., Kluger, Y., and Reinberg, D. (2012). PCGF homologs, CBX proteins, and RYBP define functionally distinct PRC1 family complexes. Mol. Cell *45*, 344–356.

Hammer, G.E., and Ma, A. (2013). Molecular control of steady-state dendritic cell maturation and immune homeostasis. Annu. Rev. Immunol. *31*, 743–791.

Huang, Y., Min, S., Lui, Y., Sun, J., Su, X., Liu, Y., Zhang, Y., Han, D., Che, Y., Zhao, C., et al. (2012). Global mapping of H3K4me3 and H3K27me3 reveals chromatin state-based regulation of human monocyte-derived dendritic cells in different environments. Genes Immun. *13*, 311–320.

Johnson, D.J., and Ohashi, P.S. (2013). Molecular programming of steady-state dendritic cells: impact on autoimmunity and tumor immune surveillance. Ann. N Y Acad. Sci. *1284*, 46–51.

Kane, C.M., Cervi, L., Sun, J., McKee, A.S., Masek, K.S., Shapira, S., Hunter, C.A., and Pearce, E.J. (2004). Helminth antigens modulate TLR-initiated dendritic cell activation. J. Immunol. *173*, 7454–7461.

Krawczyk, C.M., Sun, J., and Pearce, E.J. (2008). Th2 differentiation is unaffected by Jagged2 expression on dendritic cells. J. Immunol. *180*, 7931–7937.

Krawczyk, C.M., Holowka, T., Sun, J., Blagih, J., Amiel, E., DeBerardinis, R.J., Cross, J.R., Jung, E., Thompson, C.B., Jones, R.G., and Pearce, E.J. (2010). Toll-like receptor-induced changes in glycolytic metabolism regulate dendritic cell activation. Blood *115*, 4742–4749.

Lauberth, S.M., Nakayama, T., Wu, X., Ferris, A.L., Tang, Z., Hughes, S.H., and Roeder, R.G. (2013). H3K4me3 interactions with TAF3 regulate preinitiation complex assembly and selective gene activation. Cell *152*, 1021–1036.

Lee, M.G., Norman, J., Shilatifard, A., and Shiekhattar, R. (2007). Physical and functional association of a trimethyl H3K4 demethylase and Ring6a/MBLR, a polycomb-like protein. Cell *128*, 877–887.

Li, H., and Durbin, R. (2009). Fast and accurate short read alignment with Burrows-Wheeler transform. Bioinformatics *25*, 1754–1760.

Macagno, A., Napolitani, G., Lanzavecchia, A., and Sallusto, F. (2007). Duration, combination and timing: the signal integration model of dendritic cell activation. Trends Immunol. *28*, 227–233.

Mäkelä, S.M., Strengell, M., Pietilä, T.E., Österlund, P., and Julkunen, I. (2009). Multiple signaling pathways contribute to synergistic TLR ligand-dependent cytokine gene expression in human monocyte-derived macrophages and dendritic cells. J. Leukoc. Biol. *85*, 664–672.

Memari, B., Bouttier, M., Dimitrov, V., Ouellette, M., Behr, M.A., Fritz, J.H., and White, J.H. (2015). Engagement of the aryl hydrocarbon receptor in mycobacterium tuberculosis-infected macrophages has pleiotropic effects on innate immune signaling. J. Immunol. *195*, 4479–4491.

Mogensen, T.H. (2009). Pathogen recognition and inflammatory signaling in innate immune defenses. Clin. Microbiol. Rev. *22*, 240–273.

Muramoto, T., Müller, I., Thomas, G., Melvin, A., and Chubb, J.R. (2010). Methylation of H3K4 Is required for inheritance of active transcriptional states. Curr. Biol. *20*, 397–406.

Outchkourov, N.S., Muiño, J.M., Kaufmann, K., van Ijcken, W.F., Groot Koerkamp, M.J., van Leenen, D., de Graaf, P., Holstege, F.C., Grosveld, F.G., and Timmers, H.T. (2013). Balancing of histone H3K4 methylation states by the Kdm5c/SMCX histone demethylase modulates promoter and enhancer function. Cell Rep. *3*, 1071–1079.

Paddison, P.J., Cleary, M., Silva, J.M., Chang, K., Sheth, N., Sachidanandam, R., and Hannon, G.J. (2004). Cloning of short hairpin RNAs for gene knockdown in mammalian cells. Nat. Methods *1*, 163–167.

Ruthenburg, A.J., Allis, C.D., and Wysocka, J. (2007). Methylation of lysine 4 on histone H3: intricacy of writing and reading a single epigenetic mark. Mol. Cell *25*, 15–30.

Sallusto, F., Cella, M., Danieli, C., and Lanzavecchia, A. (1995). Dendritic cells use macropinocytosis and the mannose receptor to concentrate macromolecules in the major histocompatibility complex class II compartment: downregulation by cytokines and bacterial products. J. Exp. Med. *182*, 389–400.

Schuettengruber, B., Chourrout, D., Vervoort, M., Leblanc, B., and Cavalli, G. (2007). Genome regulation by polycomb and trithorax proteins. Cell *128*, 735–745.

Sun, J., Wang, J., He, L., Lin, Y., and Wu, J. (2015). Knockdown of polycomb-group RING finger 6 modulates mouse male germ cell differentiation in vitro. Cell. Physiol. Biochem. *35*, 339–352.

Wen, H., Dou, Y., Hogaboam, C.M., and Kunkel, S.L. (2008a). Epigenetic regulation of dendritic cell–derived interleukin-12 facilitates immunosuppression after a severe innate immune response. Blood *111*, 1797–1804.

Wen, H., Schaller, M.A., Dou, Y., Hogaboam, C.M., and Kunkel, S.L. (2008b). Dendritic cells at the interface of innate and acquired immunity: the role for epigenetic changes. J. Leukoc. Biol. *83*, 439–446.

Yang, H., Qiu, Q., Gao, B., Kong, S., Lin, Z., and Fang, D. (2014). Hrd1-mediated BLIMP-1 ubiquitination promotes dendritic cell MHCII expression for CD4 T cell priming during inflammation. J. Exp. Med. *211*, 2467–2479.

Yang, C.-S., Chang, K.-Y., Dang, J., and Rana, T.M. (2016). Polycomb group protein Pcgf6 acts as a master regulator to maintain embryonic stem cell identity. Sci. Rep. *6*, 26899.

Yoshimoto, T., Nagase, H., Ishida, T., Inoue, J., and Nariuchi, H. (1997). Induction of interleukin-12 p40 transcript by CD40 ligation via activation of nuclear factor-kappaB. Eur. J. Immunol. *27*, 3461–3470.

Yu, H.-B., Yurieva, M., Balachander, A., Foo, I., Leong, X., Zelante, T., Zolezzi, F., Poidinger, M., and Ricciardi-Castagnoli, P. (2015). NFATc2 mediates epigenetic modification of dendritic cell cytokine and chemokine responses to dectin-1 stimulation. Nucleic Acids Res. *43*, 836–847.

Zdzieblo, D., Li, X., Lin, Q., Zenke, M., Illich, D.J., Becker, M., and Müller, A.M. (2014). Pcgf6, a polycomb group protein, regulates mesodermal lineage differentiation in murine ESCs and functions in iPS reprogramming. Stem Cells *32*, 3112–3125.

Zhang, Y., Liu, T., Meyer, C.A., Eeckhoute, J., Johnson, D.S., Bernstein, B.E., Nusbaum, C., Myers, R.M., Brown, M., Li, W., and Liu, X.S. (2008). Model-based analysis of ChIP-seq (MACS). Genome Biol. *9*, R137.